

Hyperbaric Oxygen Attenuates Apoptosis and Decreases Inflammation in an Ischemic Wound Model

Qixu Zhang¹, Qing Chang¹, Robert A. Cox², Xuemei Gong¹ and Lisa J. Gould¹

The molecular mechanisms whereby hyperbaric oxygen (HBO) improves ischemic wound healing remain elusive. In this study, a rat model of wound ischemia was used to test the hypothesis that HBO enhances wound healing by modulating hypoxia-inducible factor-1 α (HIF-1 α) signaling. Male Sprague-Dawley rats underwent creation of a previously validated ischemic flap. Three groups underwent daily treatment: HBO (90 minutes, 2.4 atm); systemic administration of the free radical scavenger, *N*-acetylcysteine (NAC 150 mg kg⁻¹ intraperitoneal); control (neither HBO nor NAC). HBO treatment improved healing of the ischemic wounds. Analysis of ischemic wound tissue extracts demonstrated significantly reduced expression of HIF-1 α , p53, and Bnip3. Additionally, HBO increased expression of Bcl-2 while decreasing cleaved caspase-3. DNA fragmentation was abolished and the number of TUNEL-positive cells was reduced compared to the other groups. Vascular endothelial growth factor, cyclooxygenase-2, and neutrophil infiltration were reduced in ischemic wounds treated with HBO. These results indicate that HBO improves ischemic wound healing by downregulation of HIF-1 α and subsequent target gene expression with attenuation of cell apoptosis and reduction of inflammation.

Journal of Investigative Dermatology advance online publication, 13 March 2008; doi:10.1038/jid.2008.53

INTRODUCTION

Chronic wounds are a common but underrecognized problem that significantly impacts patients' quality of life. The wide range of therapeutic options for these wounds indicates that the mechanisms responsible for non-healing wounds are poorly understood. Hyperbaric oxygen therapy (HBOT) has been used to treat chronic wounds for about 40 years on the assumption that delivery of increased oxygen to the wound will improve healing. Several randomized, controlled trials have shown the benefit of HBOT in diabetic foot ulcer outcome as measured by reduction in the risk of major amputation (Doctor *et al.*, 1992; Faglia *et al.*, 1996; Kalani *et al.*, 2002; Abidia *et al.*, 2003; Kessler *et al.*, 2003), and yet the effect on actual ulcer healing remains elusive. Treatment of chronic wounds other than diabetic foot wounds with HBOT has not withstood the rigor of randomized controlled trials, perhaps because the heterogeneity of wounds other than diabetic foot ulcers makes such

trials extremely difficult to perform (Kranke *et al.*, 2004). Thus, the utility of HBOT for healing chronic wounds remains a subject of debate. On the other hand, HBOT has been shown to protect the central nervous system from ischemia or ischemia-reperfusion injury (Baidin *et al.*, 1997; Rosenthal *et al.*, 2003). Cited mechanisms for HBO-induced neuroprotection include increased oxygen supply (Sunami *et al.*, 2000), improved cerebral metabolism (Ginsberg, 2003), reduced inflammation (Thom, 1993), attenuation of apoptosis (Calvert *et al.*, 2003; Yin *et al.*, 2003), and ischemic tolerance or ischemic preconditioning (Xiong *et al.*, 2000; Dong *et al.*, 2002). These beneficial effects suggest that oxygen has multiple roles when delivered in high concentrations to an ischemic environment. It is our premise that improved understanding of the effect of oxygen on ischemic wounds will lead to more effective, specifically targeted wound treatments.

Hypoxia-inducible factor-1 (HIF-1) plays a central role in oxygen homeostasis through a redox-dependent mechanism. Numerous studies have shown that HIF-1 α and its target genes play an important role in cardiac myocyte death and brain death caused by hypoxia (Regula *et al.*, 2002; Yussman *et al.*, 2002; Graham *et al.*, 2004; Li *et al.*, 2005; Ostrowski *et al.*, 2005; Galvez *et al.*, 2006), and yet the effect of extreme hyperoxia, which also increases free radicals, is unclear. We proposed that HBO would regulate HIF-1 through increased free radical oxygen species and that regulation of HIF-1 α -associated genes would play an important role in the ischemic wound healing process. In this study, we examine the effect of HBO and the free radical scavenger *N*-acetylcysteine

¹Division of Plastic Surgery, Department of Surgery, University of Texas Medical Branch, Galveston, Texas, USA and ²Department of Pathology, University of Texas Medical Branch, Galveston, Texas, USA

Correspondence: Dr Lisa J. Gould, Department of Surgery, University of South Florida, James A. Haley Veterans Hospital, Tampa, Florida 33612, USA. E-mail: lisa.gould@va.gov

Abbreviations: COX-2, cyclooxygenase-2; HBO, hyperbaric oxygen; HBOT, hyperbaric oxygen therapy; HIF-1 α , hypoxia-inducible factor-1 α ; NAC, *N*-acetylcysteine; PscO₂, subcutaneous tissue oxygen tension; TBST, Tris-buffered saline with Tween-20; VEGF, vascular endothelial growth factor

Received 27 June 2007; revised 8 November 2007; accepted 20 December 2007

(NAC) on HIF-1 α expression, cell apoptosis, and apoptosis-related gene products in an ischemic wound model (Gould et al., 2005).

RESULTS

Ischemic wound healing is improved by HBO

All of the flaps survived completely without necrosis. As shown in Figure 1a, ischemic wounds in the HBO-treated rats were smaller than those in all other groups at each time point. HBO treatment significantly reduced wound size on day 7 compared with NAC ($P<0.05$), and on day 10 compared with NAC and control ($P<0.05$). The non-ischemic wounds healed notably faster than ischemic wounds, indicating that ischemia clearly impairs wound healing and that the ischemic wound model is reliable and reproducible as reported previously (Gould et al., 2005). In the non-ischemic wounds, HBO appears to have a marked effect on wound size between days 0 and 3. We originally thought that this was a spurious result; however, HBO has been shown to enhance epithelial proliferation and migration in the human skin equivalent model, as reported by Kairuz et al. (2007). The effect in that *in vitro* model is short lived and may explain why the difference is noted only at day 3 in our model.

Prolonged hypoxia induces transcription factor HIF-1 α

HIF-1 α expression increased in all groups, peaking on day 7 and decreasing thereafter. As shown in Figure 2a and b, HBO significantly decreased HIF-1 α expression on day 7 ($P<0.05$). On the other hand, NAC treatment markedly induced HIF-1 α expression up to day 10, a significant difference from the other two groups ($P<0.05$). This pattern of HIF-1 α expression indicates that HBO improves ischemic wound tissue oxygen

supply and protects against hypoxic stress. HIF-1 α expression was much lower in the non-ischemic wound tissue than that in the ischemic wound tissue (Figure 2c and d). As shown in Figure 2e, strong HIF-1 α staining was detected in the nuclei of cells, indicating that in ischemic tissue, HIF-1 α is translocated to the nucleus, allowing activation of target gene transcription. Nuclear staining is less apparent in non-ischemic wound tissue (Figure 2f).

HBOT decreased vascular endothelial growth factor expression and inflammation

Vascular endothelial growth factor (VEGF) expression was induced in the ischemic wound tissue of all groups. Correlating with HIF-1 α , VEGF expression peaked on day 7 and was sustained through day 10 (Figure 3a). Compared to NAC and control groups, HBO significantly reduced VEGF protein level at day 7 ($P<0.05$). The result was confirmed by immunohistochemistry (Figure 3b–e). Strongly positive VEGF staining was seen in the epidermis, dermis, and ischemic wound granulation tissue in the NAC and control groups. HBO significantly decreased the number of neutrophils in the wound granulation tissue (Figure 4c). Expression of the inflammatory marker cyclooxygenase-2 (COX-2) (Seibert et al., 1995; Nathan, 2002) was also reduced dramatically by HBOT at day 7 (Figure 4a and b). These data indicate that HBOT reduces the inflammatory response in ischemic wound tissue.

p53 and BNip3 protein levels are induced in ischemic wound tissue and decreased by HBOT

As shown in Figure 5, p53 increased in the ischemic wound tissue from days 3 to 10. At each time point, HBO decreased p53 protein expression in the period of wound healing compared to other groups.

As a member of the Bcl-2 family, BNip3 is likely to be a direct target gene for HIF-1 α (Bruick, 2000; Greijer et al., 2005). We therefore assessed whether BNip3 was upregulated in a manner consistent with HIF-1 α in the ischemic-hypoxic wound tissue. As shown in Figure 6a and b, 60 kDa BNip3 was identified after 3 days of wound ischemia. In the NAC and control groups, BNip3 was strongly expressed during the entire post-ischemic period. In the HBO treatment group, BNip3 was highly expressed on day 3 but markedly reduced by day 7, and was present at low levels on days 10 and 14. Compared to the other two groups, HBO significantly reduced BNip3 expression on days 7 and 10 ($P<0.05$). As shown in Figure 6c and d, the lactate level was higher in the ischemic wound tissue between days 3 and 14, indicative of acidosis. Acidosis is known to be required for activation and stabilization of the BNip3 protein (Graham et al., 2004).

HBOT increased Bcl-2 expression and the Bcl-2/Bax ratio

BNip3 has been shown to form heterodimers with Bcl-2 and Bcl-xl, which are antiapoptotic Bcl-2 family members. We next analyzed expression of these two factors. As shown in Figure 7, HBO dramatically increased Bcl-2 expression at each time point compared to the other two groups ($P<0.05$). The control group had a relatively lower level Bcl-2 expression

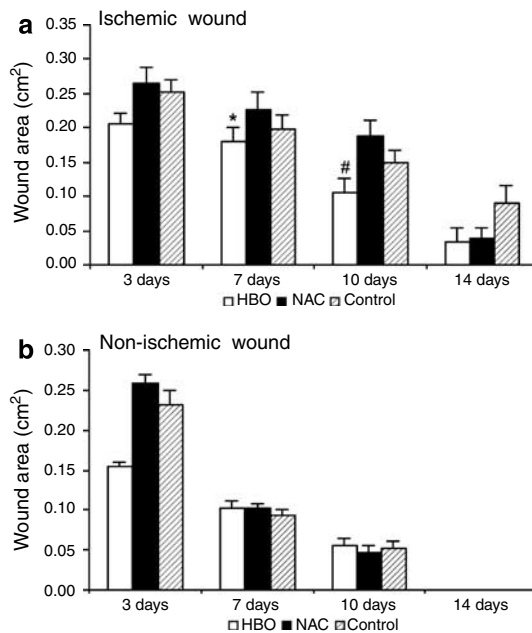


Figure 1. Wound surface area. (a) HBO-treated ischemic wounds healed faster than all other groups. * $P<0.05$, HBO versus NAC; # $P<0.05$, HBO versus NAC and control. (b) There was no significant difference between groups in non-ischemic wounds.

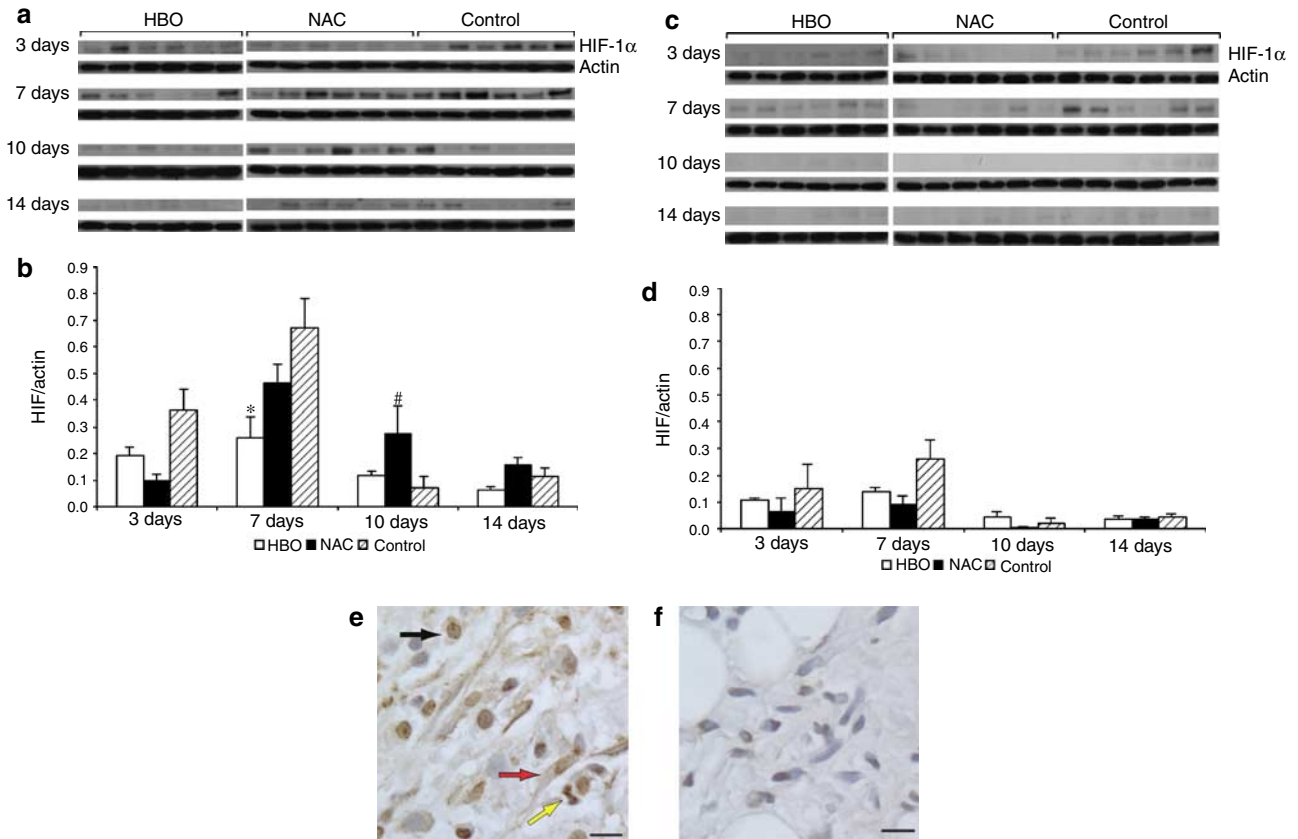


Figure 2. HIF-1 α expression in ischemic and non-ischemic wounds. (a) Western blot shows the expression of HIF-1 α and corresponding β -actin in the ischemic wound tissue from six animals in each group at each time point. (A representative of three separate blots is shown.) (b) Densitometry analysis shows that HIF-1 α expression increased further in the post-ischemic period, peaked on day 7, and decreased thereafter. HBO significantly decreased HIF-1 α expression on day 7 (* P <0.05, HBO versus NAC and control). NAC treatment markedly induced HIF-1 α expression and lasted for 10 days ([#] P <0.05, NAC versus HBO and control). (c) HIF-1 α and corresponding β -actin bands for non-ischemic wound samples (representative blot). (d) HIF-1 α expression increased in the post-wound period, peaked on day 7, and decreased thereafter. There was no significant difference between HBO and control. HIF-1 α expression was markedly lower than in ischemic wound tissue. (e) Strong HIF-1 α staining was detected in the nuclei of fibroblasts (gray arrow), macrophages (black arrow), and endothelial cells (white arrow) in ischemic wound tissue. (f) Minimal HIF-1 α staining was detected in non-ischemic wound tissue with fewer positive nuclei. Bars = 20 μ m.

from day 7 to day 14, whereas NAC treatment significantly inhibited Bcl-2 throughout the time course. Unlike Bcl-2, Bcl-xl was strongly expressed in all groups and at each time point. There was no significant difference between the three groups (data not shown), nor was there a significant difference in the expression of proapoptotic Bax (data not shown). The Bcl-2/Bax ratio was markedly increased by HBO treatment at each time point as shown in Figure 7c.

HBOT decreased active caspase-3 expression and attenuated apoptosis in ischemic wound tissue

Caspase-3 is a common and reliable apoptotic marker, hence we next assessed whether HBO decreased its expression. As shown in Figure 8a and b, HBO significantly decreased cleaved caspase-3 expression at each time point (P <0.05). This result was confirmed by immunohistochemistry. As shown in Figure 9a-f, strongly positive staining for cleaved caspase-3 was seen in the epidermis and dermis of ischemic wound tissue in the NAC and control groups. HBO significantly decreased cleaved caspase-3-positive cell numbers in the wound tissue.

TUNEL technique allows the visualization of cell nuclei containing fragmented DNA, a typical feature of apoptosis. Positive TUNEL-stained cells were detected in the dermis and hypodermis of ischemic wound tissue during wound healing in all groups. As shown in Figure 10a, c, and e, the TUNEL-positive cell number was significantly decreased by HBO treatment on days 7 and 14 compared to the other two groups (P <0.05 and P <0.01, respectively). There was a significant difference between HBO and NAC groups on day 10 (P <0.05). The DNA-specific fluorochrome Hoechst 33258 was used to analyze the nuclear morphology after TUNEL staining. These slides were analyzed for apoptotic features such as chromatin condensation and nuclear fragmentation (von Kobyletzki *et al.*, 2000). As shown in Figure 10b, d, and f, most of the TUNEL-positive cells stained with Hoechst 33258 revealed an increase in intensity of nuclear fluorescence by changing their fluorescence characteristics from dark blue (normal cells) to a light blue/white color, indicating chromatin condensation.

In addition to TUNEL staining, genomic DNA electrophoresis shows only one sample in the HBO-treated group

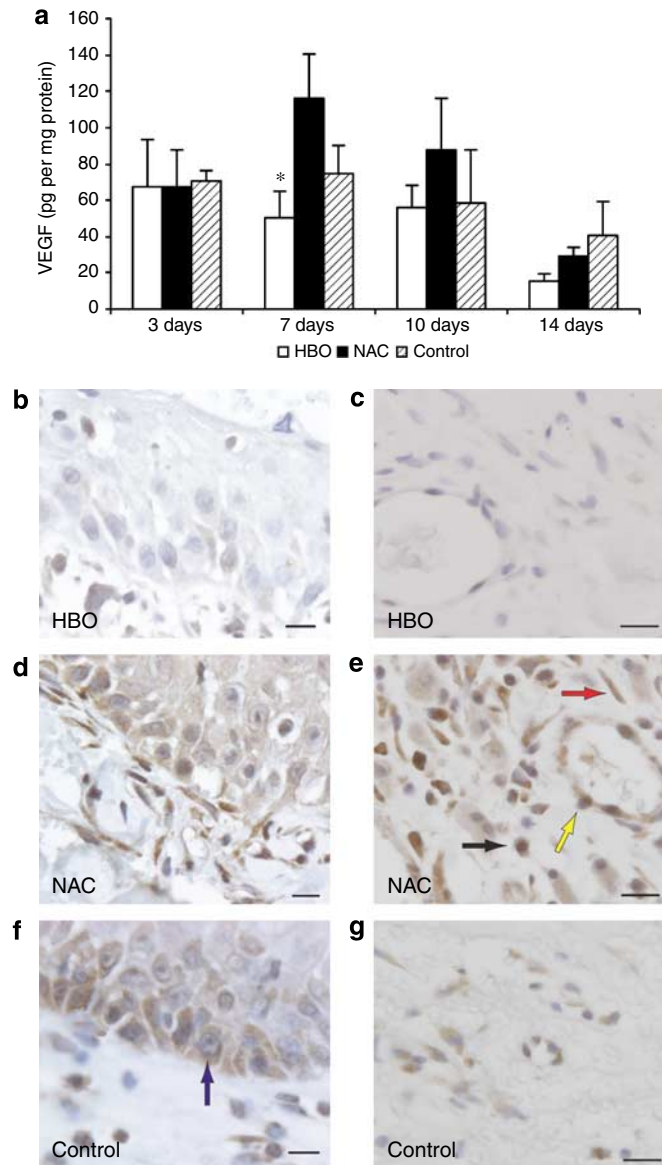


Figure 3. VEGF expression in ischemic wound tissue. (a) ELISA result shows that VEGF expression was induced in the ischemic wound tissue in all groups. It peaked on day 7, lasted up to day 10, and decreased significantly by day 14. HBO significantly reduced VEGF protein level on day 7 compared to NAC and control (**P*<0.05, *n*=6). VEGF staining in the (b, d, and f) epidermis and (c, e, and g) dermis. Strongly positive VEGF immunostaining was seen in the epidermis and dermis of ischemic wound tissue in (d, e) NAC-treated wounds and (f, g) control. VEGF was expressed predominantly in the endothelial cells (e, white arrow), fibroblast cells (e, gray arrow), macrophage cells (e, black arrow), and keratinocytes (f, arrow). (b, c) The number of VEGF-positive cells was decreased by HBO. Bars = 20 μm.

that showed a clear DNA ladder. However, there were four samples with a clear DNA ladder in the NAC treatment group and three in the control group (Figure 11). These data clearly indicate that cell apoptosis is reduced in the HBO treatment group compared to the other two groups.

HBO effects on cell DNA synthesis

BrdU incorporation into the wound tissue DNA was detected by the quantitative DNA dot-blotting method. As shown

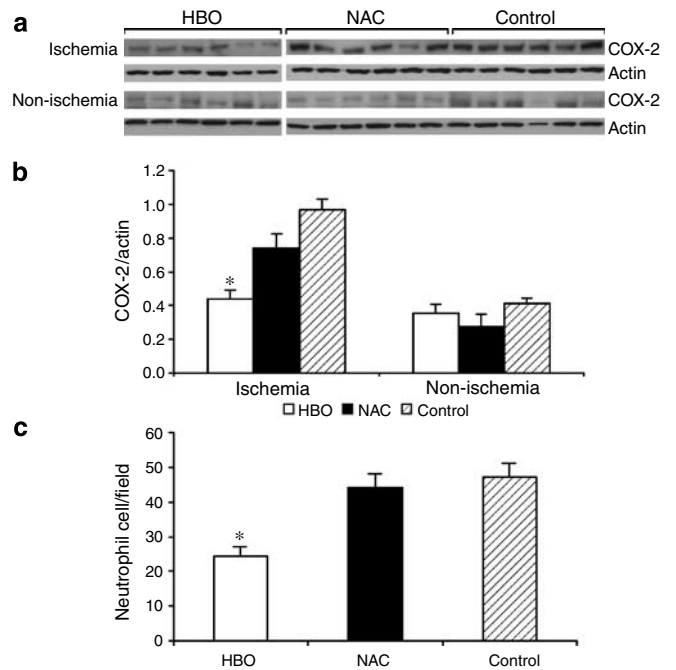


Figure 4. COX-2 expression in ischemic wound tissue. (a) Western blot shows the expression of COX-2 and corresponding β-actin in the wound tissue from six animals in each group at day 7 (representative blot). (b) Densitometry analysis shows that HBO significantly decreased COX-2 expression compared to NAC and control (**P*<0.05). COX-2 expression was low in the non-ischemic wound tissue, with no difference between groups. (c) HBO significantly reduced the number of neutrophils in ischemic wound tissue at day 7 (**P*<0.05).

in Figure 12a and b, a strong BrdU signal was detected in DNA from six samples in HBO and five samples in the control group at day 10. Densitometric analysis showed no significant difference between these groups. However, NAC significantly decreased BrdU incorporation in ischemic wound tissue (*P*<0.05). There was no significant difference between the three groups in the non-ischemic wound tissue. These data indicate that HBO has minimal effect on the induction of cellular DNA synthesis. We have confirmed these results by immunohistochemistry for proliferating cell nuclear antigen and by western blotting for phosphoinositide-3 kinase protein expression (see Supplementary Materials, Figures S1 and S2).

DISCUSSION

The two major findings from this work are that treatment of ischemic wounds with HBO reduced apoptotic cell death without a corresponding increase in proliferation, and that HBO treatment reduced inflammation in the ischemic wound. To the best of our knowledge, this is the first study to look at these parameters in ischemic wounds *in vivo*. The ischemic flap utilized in this study is designed to create prolonged ischemia of the tissue in and around the wound. We have previously shown that the average subcutaneous tissue oxygen tension (*P*_{scO₂}) at the wound edge is only 30 mm Hg (based on polarographic measurements) (Gould *et al.*, 2005). Thus, even the wound margins in this excisional

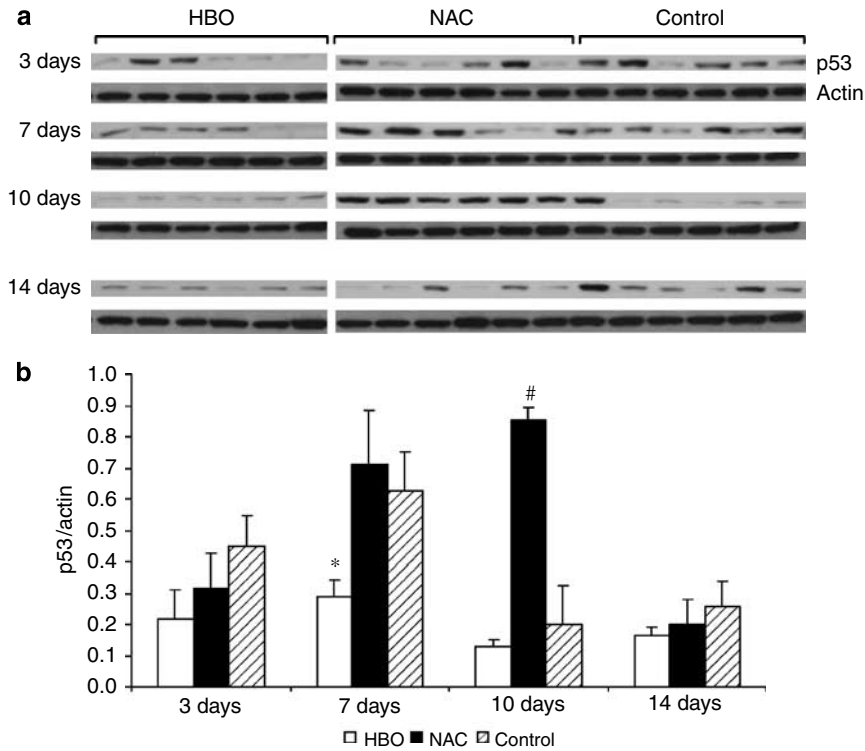


Figure 5. p53 expression in ischemic wounds over time. (a) Western blot shows the expression of p53 and corresponding β -actin in the ischemic wound tissue for all samples (representative blot). (b) Densitometry analysis shows that p53 expression increased in the post-ischemic period, peaked on day 7, and decreased thereafter. HBO significantly decreased p53 expression on day 7 ($*P < 0.05$). NAC treatment markedly induced p53 expression with the greatest difference on day 10 ($^{\#}P < 0.01$).

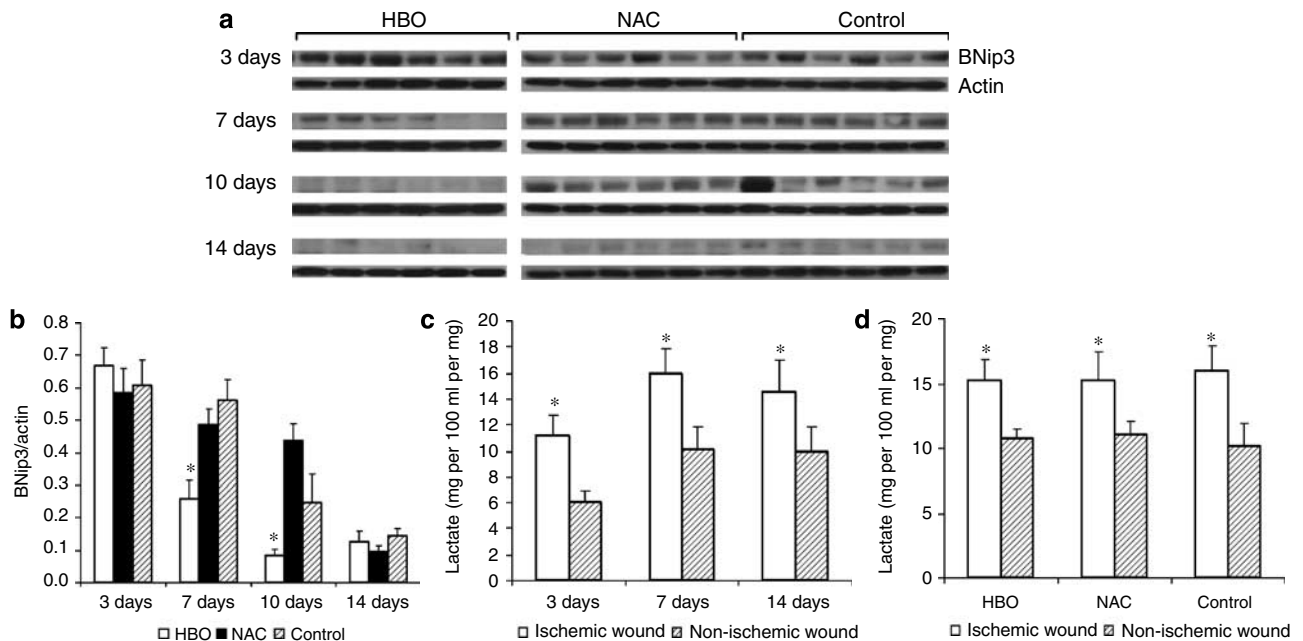


Figure 6. BNip3 expression and lactate levels in ischemic wounds. (a) Western blot shows the expression of BNip3 and corresponding β -actin in the ischemic wound tissue for all samples (representative blot). (b) Densitometry analysis shows that BNip3 expression increased in the post-ischemic period, peaked on day 7, and decreased thereafter. HBO significantly decreased BNip3 expression on days 7 and 10 ($*P < 0.05$). (c) L-Lactate was determined spectrophotometrically at 340 nm using a commercially available kit (Sigma-Aldrich), which follows the production of NADH. The lactate level increased in ischemic compared to non-ischemic wound tissue at all time points in the control group ($*P < 0.05$). (d) The lactate level was significantly elevated in ischemic compared to non-ischemic wound tissue on day 7 in all treatment groups. NADH, nicotinamide adenine dinucleotide ($*P < 0.05$).

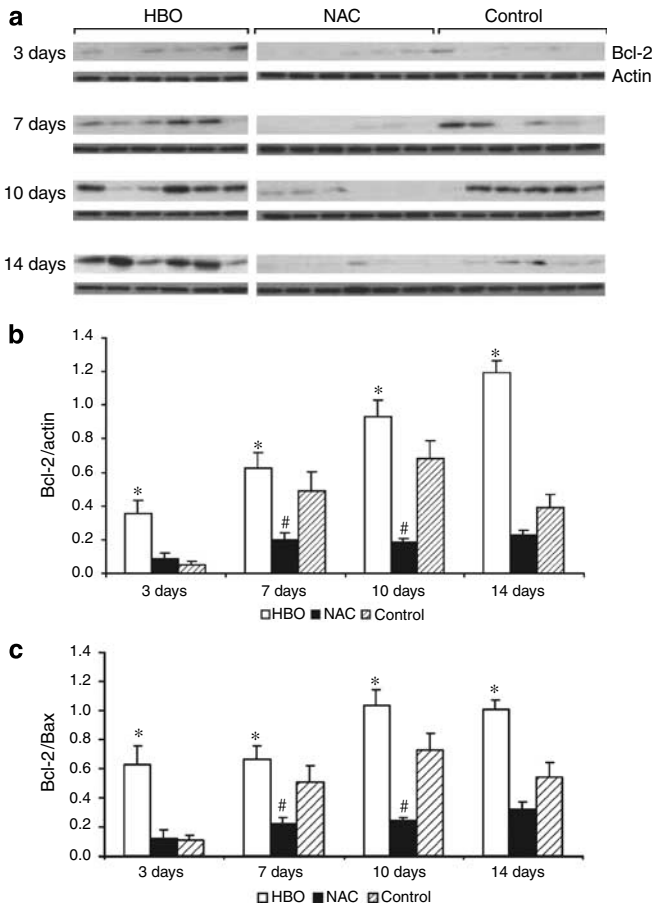


Figure 7. Expression of anti-apoptotic marker Bcl-2 in ischemic wound tissue. (a) Western blot shows the expression of Bcl-2 in the ischemic wound tissue from six animals in each group at each time point. (b) HBO dramatically increased Bcl-2 expression in each time point compared to the other two groups (* $P < 0.05$). NAC significantly decreased Bcl-2 level compared to control on days 7 and 10 (* $P < 0.05$). (c) The Bcl-2/Bax ratio was markedly increased by HBO treatment at each time point (* $P < 0.05$). NAC significantly decreased the Bcl-2/Bax ratio compared to control (* $P < 0.05$).

wound model are critically hypoxic, mimicking the clinical scenario of a wound on an ischemic limb. In this study, we demonstrate that this hypoxic environment results in prolonged elevation of HIF-1 α and associated downstream signals, including p53 and BNip3, resulting in increased apoptosis. Therefore, although hypoxia is an essential signal during normal wound healing, this signaling may be detrimental when the wound is surrounded by an ischemic environment.

We have shown that HBO increased the rate of wound healing in the ischemic wounds but not in the non-ischemic wounds. In conditions of high oxygen, HIF-1 α is degraded by an oxygen-dependent prolyl hydroxylase. We therefore hypothesized that HIF-1 α and subsequent downstream signaling, including apoptosis, would be reduced by HBO. This study confirms that hypothesis: HBO decreased HIF-1 α protein expression significantly as well as p53, BNip3, and VEGF at days 7 and 10. Surprisingly, this effect was not apparent before day 7. One potential explanation for that is the intermittent nature of HBO treatment. In the ischemic rabbit ear model, it has been shown that in the first days of

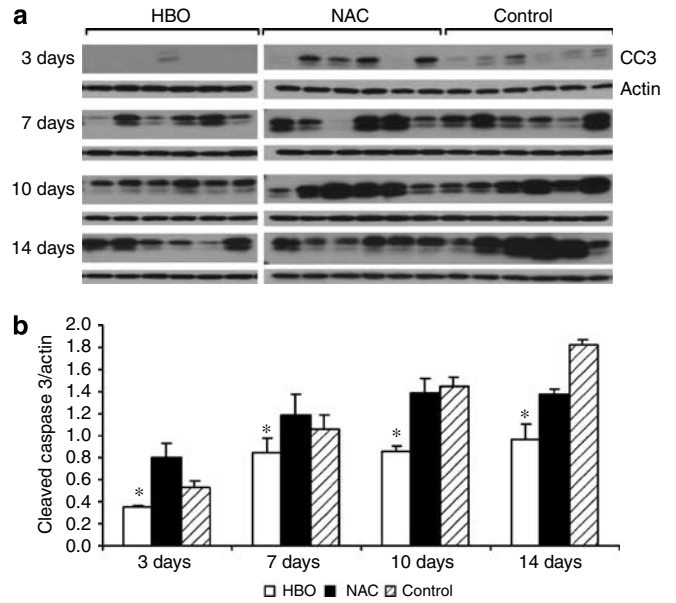


Figure 8. Expression of cleaved caspase-3 as a marker of apoptosis. (a) Western blot analysis shows the expression of cleaved caspase-3 (CC3) in the ischemic wound tissue from all samples. (b) HBO significantly reduced cleaved caspase-3 expression at each time point. (* $P < 0.05$ compared to control.)

HBO treatment, the P_{scO_2} of ischemic tissue increases to a mean of 312 ± 45 mmHg and remains elevated for about 4 hours. After 14 days of treatment, although the baseline tissue P_{scO_2} is not significantly greater, the mean plateau with treatment is higher (507 mmHg), with a more rapid return to baseline (0.7 hours) (Siddiqui *et al.*, 1997). The authors suggest that this is due to increased tissue responsiveness, possibly due to a relative increase in blood flow in the ischemic region in direct proportion to the cumulative number of treatments. In fact, they show that the rapid return to baseline after HBO treatment occurs by day 7, concurrent with our data indicating diminished HIF-1 α within the wound bed. This suggests that increased oxygen is reaching the entire wound bed, resulting in degradation of HIF-1 α during the period of hyperoxia.

In contrast to our results, Sheikh *et al.* (2000) have demonstrated increased VEGF at 5 days of HBOT treatment. This model has a couple of critical differences that may explain the opposing results. Wound fluid is sampled from a cylinder instead of the actual tissue. Thus, only secreted proteins from tissue that is well perfused are sampled. Shenberger *et al.* (2007) have demonstrated that hyperoxia decreases lung VEGF mRNA expression while increasing VEGF protein within the epithelial lining fluid by stimulating the release of VEGF from cell-associated stores. Similarly, the adult retina responds to hyperoxia with reduced expression of VEGF and pruning of immature vessels (Yamada *et al.*, 1999; Dor *et al.*, 2001). Thus, we believe that the difference lies in the fact that we examine tissue VEGF, whereas the model of Sheikh *et al.* (2000) looks only at secreted proteins. Because it is not practical for us to collect wound fluid in this model, further studies that examine tissue VEGF mRNA might reconcile the difference. Although not studied in detail in a

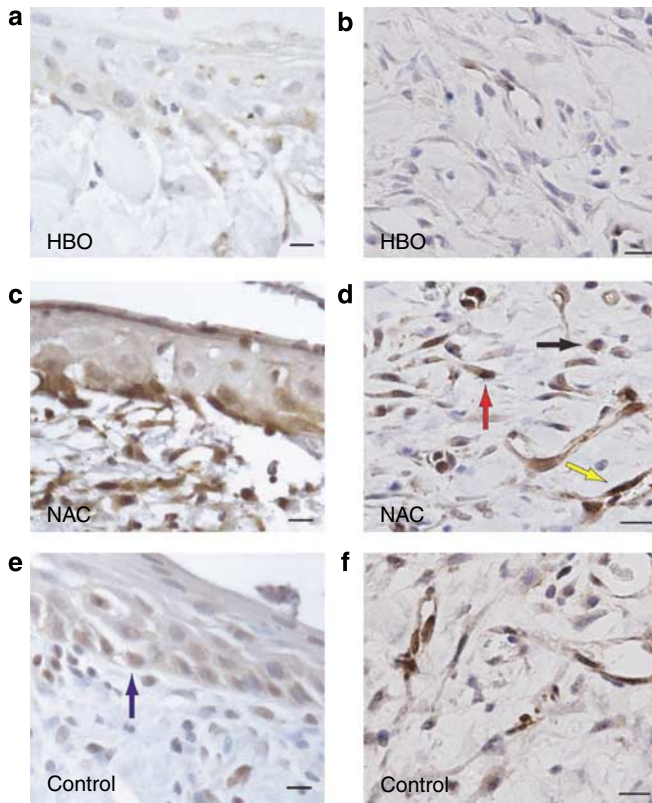


Figure 9. Localization of cleaved caspase-3. Immunohistochemistry shows strongly positive staining for cleaved caspase-3 in the (c, e) epidermis and (d, f) dermis of ischemic wound tissue in the NAC and control groups. Cleaved caspase-3 was expressed predominantly in the endothelial cells (d, white arrow), fibroblasts (d, gray arrow), and macrophages (d, black arrow), especially in the dermal and hypodermal layers, and in the keratinocytes (e, arrow). HBO significantly decreased cleaved caspase-3-positive cell numbers in the (a) epidermis and (b) dermis of wound tissue. Bars = 20 μ m.

wound model, alternating periods of hyperoxia and hypoxia in the retina create a very different environment compared to continuous hyperoxia (Werdich *et al.*, 2004). Furthermore, work by Hopf *et al.* (2005) has clearly shown a dose dependence of oxygen therapy. In our model, ischemic wounds receive once daily HBOT, resulting in marked fluctuations between hyperoxia and hypoxia, whereas in Sheikh's model HBO treatments are twice daily and VEGF sampling is between the two treatments. Cylinder oxygen measurements indicate that the oxygen tension may not return to baseline between treatments, resulting in a condition of near-continuous hyperoxia.

HIF-1 α has been rigorously shown to play a role in hypoxia-mediated apoptosis via two mechanisms (Carmeliet *et al.*, 1998). HIF-1 α binds to Mdm2, which enhances the creation of a stable HIF-1 α -p53 complex, leading to activation of p53-mediated transcription in cells (Chen *et al.*, 2003; Greijer and van der Wall, 2004). p53 can induce and activate the Bax and Bak proteins, which regulate the release of cytochrome *c* from the mitochondria, thereby initiating the cascade leading to apoptosis mediated by caspase-9 and caspase-3 (Wei *et al.*, 2001). Second, HIF-1 α can increase expression of BNip3, a proapoptotic member of the Bcl-2

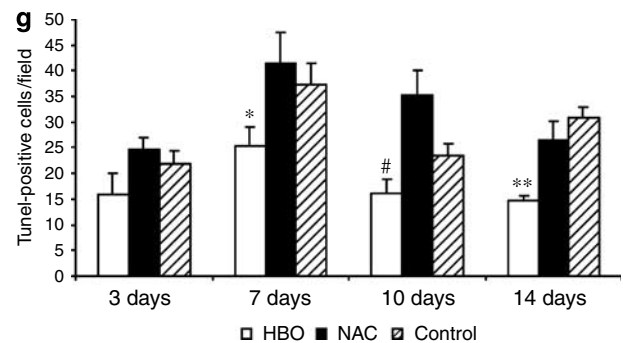
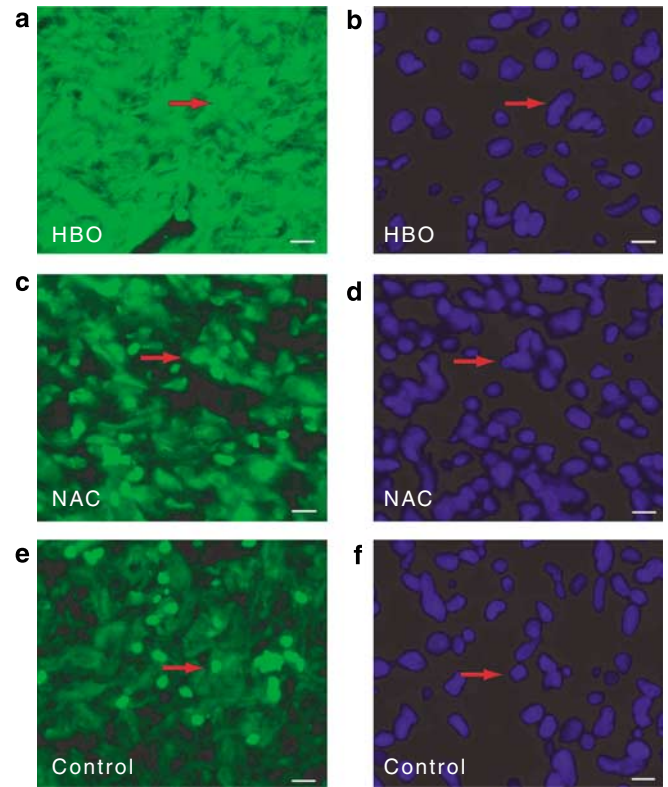


Figure 10. TUNEL and Hoechst staining of ischemic wound tissue. Apoptotic cell nuclei stained by TUNEL in the dermis of ischemic wound tissue: (a) HBO, (c) NAC, and (e) control. TUNEL-positive cell nuclei stained with Hoechst 33258 revealed brighter fluorescence by changing their fluorescence characteristics from dark blue (normal cells) to a light blue/white color due to chromatin condensation (arrow): (b) HBO; (d) NAC; (f) control. (g) TUNEL-positive cell number was significantly decreased by HBO treatment on days 7 and 14 (* P <0.05, ** P <0.01). There was a significant difference between HBO and NAC on day 10 ($^{\#}P$ <0.05). Bars = 20 μ m.

family. The BNip3 promoter contains a functional HIF-1-responsive element and is potently activated by both hypoxia and forced expression of HIF-1 α (Bruick, 2000). BNip3 has been shown to form heterodimers with antiapoptotic Bcl-2 family members, such as Bcl-2 and Bcl-xl, and may promote apoptosis by sequestering these factors (Boyd *et al.*, 1994; Yasuda *et al.*, 1998).

In this study, we show that both of these proapoptotic signaling mechanisms occur in the ischemic wound and contribute to delayed healing. Furthermore, our data support the concept that oxygen is acting as a signal transducer,

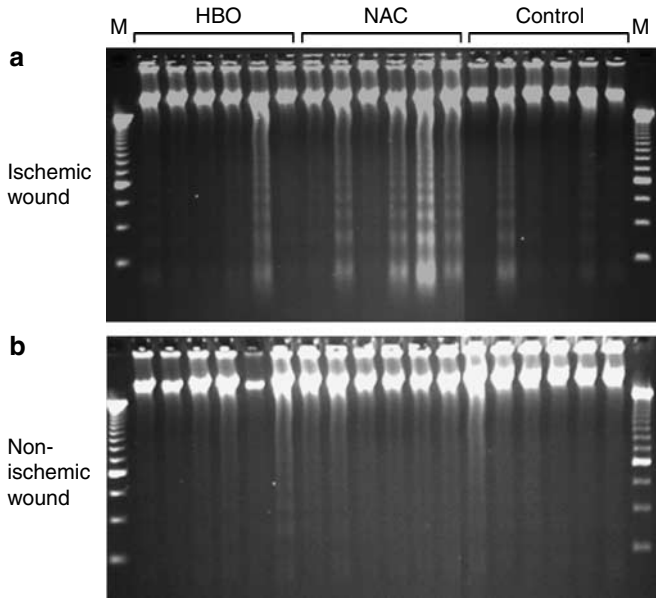


Figure 11. DNA fragmentation in ischemic and non-ischemic wounds. (a) The genomic DNA electrophoresis shows that HBO abolished DNA fragmentation compared to other groups; only one sample showed a clear DNA ladder. However, four samples in NAC treatment group and three samples in the control group had clear DNA ladders (a representative of three experiments). (b) Few DNA ladders were detected in non-ischemic wound tissue samples.

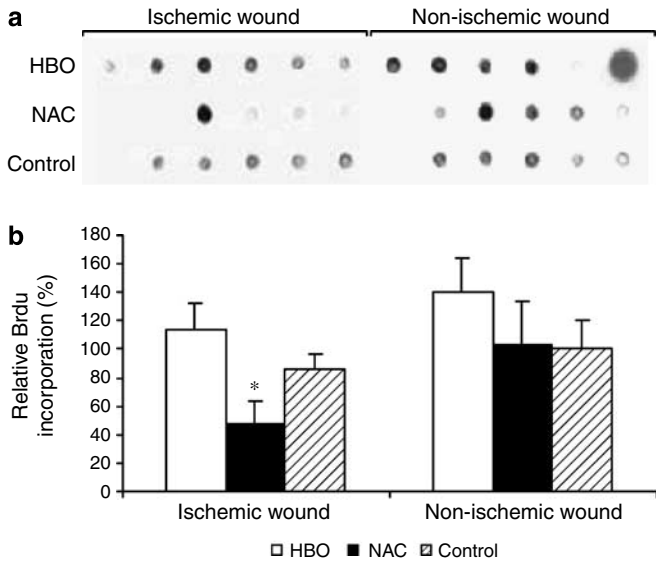


Figure 12. Cell proliferation measured by BrdU uptake in ischemic and non-ischemic wounds. (a) Strong BrdU signal was detected in DNA from six animals in HBO and five in the control group at day 10. (b) Densitometric analysis showed that in ischemic wound tissue, NAC significantly decreased BrdU incorporation (* $P < 0.05$). There was no significant difference between the three groups in non-ischemic wound tissue.

initiating a series of events that promote wound healing despite persistent hypoxia in the surrounding tissue. Specifically, HBO treatment significantly reduced HIF-1 α and p53 compared to the ischemic wounds from day 3 to day 10. In addition, BNip3 was strongly upregulated in ischemic wounds up to day 10. Concurrently, lactate in the

surrounding ischemic tissue was increased because of anaerobic glycolysis, resulting in lactic acidosis. The coexistence of ischemia-hypoxia and acidosis will activate and stabilize BNip3 protein expression. Delivery of high levels of oxygen by HBO reduced BNip3 expression and attenuated BNip3-mediated apoptosis in the wound bed despite persistently elevated lactate levels. Thus, HBO increased the antiapoptotic/proapoptotic protein ratio, resulting in reduced release of proapoptotic molecules from the mitochondria and attenuated apoptosis.

NAC is a relatively nonspecific free radical scavenger that is virtually non-toxic. Because of the ability to act as a glutathione precursor, NAC has been shown to reduce and in some cases prevent oxidant-mediated damage to cell culture or animals (Gillissen and Nowak, 1998). We anticipated that NAC would improve ischemic wound healing, hypothesizing that hypoxia would induce the mitochondria to produce free radicals in excess of the capacity of the endogenous antioxidant defense system. If NAC scavenges these excess free radicals, wound healing should improve. In fact, the effect of NAC was counter to what we expected. We confirmed this finding by using an alternative free radical scavenger. Phenyl-butyl-nitron is a nitron spin trap that forms stable adducts with carbon- and oxygen-centered radicals. In data not shown, we have demonstrated when rats with the ischemic flap were treated with and without daily phenyl-butyl-nitron for 7 days wound healing was even more severely impaired than when rats were treated with NAC. As expected, phenyl-butyl-nitron markedly reduced 3-nitrotyrosine (3-NT), but inducible nitric oxide synthase was induced above and beyond what was found in the untreated ischemic wounds. Our hypothesis is that near-complete removal of free radicals by either phenyl-butyl-nitron or NAC is detrimental to wound healing because there is a shift from apoptosis to necrotic cell death, resulting in increased inflammation and subsequent increased oxygen consumption. To clarify this as a mechanism, additional experiments in which inducible nitric oxide synthase is blocked are planned.

This finding ties in well with the second major result of this paper; that is, HBO treatment reduces inflammation in the ischemic wound. As part of the adaptive response to hypoxia, HIF-1 α activates the expression of VEGF. Increased VEGF expression stimulates endothelial cell proliferation and migration with subsequent capillary sprouting and branching to increase the delivery of oxygen and nutrients (Wang and Semenza, 1993). On the other hand, VEGF has been implicated in a variety of chronic inflammatory skin disorders, including psoriasis and neoplasms (Dvorak *et al.*, 1995; Ferrara *et al.*, 2003). In these conditions, VEGF is strongly expressed by epidermal keratinocytes, leading to increased microvascular permeability and aberrant angiogenesis (Detmar *et al.*, 1995; Ferrara *et al.*, 2003). Transgenic overexpression of VEGF in the skin results in increased density of tortuous cutaneous blood capillaries, increased numbers of mast cells, enhanced leukocyte rolling, and adhesion in post-capillary skin venules, suggesting that chronic overexpression of VEGF by the epidermis actually induces the cardinal

features of chronic skin inflammation (Detmar *et al.*, 1998). VEGF has also been shown to induce matrix metalloproteinases and nitric oxide production, increasing cell migration, vascular permeability, and inflammation (Noiri *et al.*, 1997; Lamoreaux *et al.*, 1998; Murohara *et al.*, 1998). In this study, epidermal and dermal VEGF expression was induced in all ischemic wound groups at day 3, with prolonged elevation in the control and NAC-treated groups for 10 days. We propose that persistently elevated HIF-1 α and VEGF, as seen in chronic ischemia, are detrimental to wound healing, resulting in immature vascularity and prolonged inflammation. In contrast, HBO significantly reduced HIF-1 α and VEGF protein expression by day 7, as well as neutrophil infiltration and expression of the inflammatory mediator COX-2. These data provide a molecular mechanism for improved wound healing with HBO treatment that includes controlling vascular permeability, decreasing tissue edema, and reducing inflammatory damage from tissue ischemia.

In conclusion, we have demonstrated that HBO treatment improves healing of ischemic wounds by simultaneously attenuating apoptosis and inflammation. We believe that modulation of prolonged overexpression of HIF-1 α and its target gene signal axis plays an important role in this response. Although it is unlikely that this is the only mechanism for the effect of HBO (Badr *et al.*, 2001; Dean *et al.*, 2003; Mrcic-Pelcic *et al.*, 2004; Li *et al.*, 2005; Zhang *et al.*, 2005), this is the first step in elucidating the factors and biological pathways involved in HBO-mediated healing. It is our premise that an improved understanding of these mechanisms will result in improved clinical approaches to heal these very difficult wounds.

MATERIALS AND METHODS

Antibodies anti-p53, anti-Bcl-2, anti-Bcl-xl, anti-Bax, anti-cleaved caspase-3, and anti-cyclooxygenase-2 were obtained from Cell Signaling Technology (Beverly, MA). Anti-HIF-1 α and antiproliferating cell nuclear antigen were obtained from Chemicon International (Temecula, CA), anti-BNip3 was a gift from Richard K Bruik (University of Texas Southwestern Medical Center, Dallas, TX), anti-VEGF was obtained from Biogenex (San Ramon, CA), and anti- β -actin and anti-BrdU were obtained from Sigma-Aldrich (St Louis, MO).

Ischemic tissue animal model and HBO treatment

All procedures were approved by the institution's Animal Care Committee and abided by all requirements of the Animal Welfare Act. Healthy 8-week-old male Sprague-Dawley rats (Charles River Laboratory, Wilmington, MA) weighing 250–300 g were utilized to create an ischemic wound model as described previously (Gould *et al.*, 2005). The HBO treatment was performed daily after the operation including the day of killing. The animals did not require anesthesia and breathed spontaneously during HBO treatment. The rats were placed into an HBO chamber (model number: 800-45, maximum working pressure 45 psig (2.4 atmospheres absolute); Dixie Manufacturing Co., Baltimore, MD) for 90 minutes for each treatment. After HBO treatment, the rats were placed back into the cages.

Experimental design

Seventy-two rats divided randomly into three groups underwent daily treatment: HBO (90 minutes, 2.4 atm), NAC (150 mg kg⁻¹ NAC

injected intraperitoneally), or control (neither HBO nor NAC, intraperitoneal injection of equivalent volume of saline). On days 3, 7, 10, and 14, six rats from each group were anesthetized and ischemic and non-ischemic wounds were traced on clear plastic. Wound surface area was calculated using Sigma Scan Image Software (Jandel Scientific, Corte Medera, CA). Cardiac perfusion with lactated Ringer's solution was performed and the wounds were excised for analysis. The day 10 group received an intraperitoneal injection of BrdU (50 mg per kg body weight, Sigma-Aldrich) 3 hours before killing. Non-ischemic and ischemic wounds were divided in half, with one part of the wound preserved in 10% buffered formalin for histologic analysis and the other three parts snap frozen in liquid nitrogen, stored separately at -80°C , and subsequently used for analysis of protein and DNA.

VEGF assay

Tissue stored at -80°C was homogenized by pulverization in liquid nitrogen and transferred to tissue lysis buffer (10 mM Tris-HCl, pH 7.4, 150 mM NaCl, 1% Triton X-100) plus Protease Inhibitor Cocktail (Sigma-Aldrich). Following centrifugation at 14,000 r.p.m. for 20 minutes, the supernatant was removed and stored at -70°C . VEGF levels were determined using a commercially available ELISA kit (R&D Systems, Minneapolis, MN), according to the manufacturer's instructions. Protein levels in the tissue homogenates were determined using a commercially available kit according to the BCA (bicinchoninic acid) method (Pierce Biotechnology, Rockford, IL). VEGF levels were expressed as picograms per milligram protein.

Western blot

Tissue homogenates as described above were also used for western blotting. Equal amount of protein per lane (40 μg) was separated by 4–15% SDS-PAGE (Bio-Rad, Hercules, CA) and transferred to polyvinylidene difluoride membrane (Bio-Rad). The membrane was blocked by 10% non-fat powdered milk in Tris-buffered saline with Tween-20 (TBST) (50 mM Tris-HCl, pH 7.5, 150 mM NaCl, 0.05% Tween-20). The membrane was incubated with the primary antibody in 5% non-fat milk in TBST overnight at 4°C , washed extensively with TBST, and then incubated with the secondary antibody for 40 minutes at room temperature. Bands were visualized with enhanced chemiluminescence (Amersham, Arlington Heights, IL). Relative quantities of protein were determined using a densitometer (Kodak Digital Science 1D Analysis Software, Rochester, NY) and presented in comparison with β -actin expression.

Lactate assay

Tissue was homogenized in 3 M HClO₄, transferred to tubes in a -8 to -10°C ice-salt bath, and agitated until mixed. One milliliter H₂O/0.3 ml HClO₄ was added and the suspension was mixed at 4°C for 10 minutes. Following centrifugation at 11 500 r.p.m. for 10 minutes at 4°C , the supernatant was removed and stored at -70°C . L-Lactate was determined spectrophotometrically at 340 nm using a commercially available kit (Sigma-Aldrich).

Immunohistochemistry

The tissue was fixed with 10% formalin, embedded in paraffin, and sectioned at 5 μm thickness. Sections were deparaffinized, rehydrated, and washed in distilled water. They were then placed in 95 $^{\circ}\text{C}$ antigen retrieval citrate buffer (Biogenex) in a steamer for 10 minutes. Endogenous peroxidases were blocked by incubation

with peroxide block (Innogenex, San Ramon, CA) and nonspecific binding was blocked with normal goat serum (Vector Labs, Burlingame, CA). Sections were incubated overnight with primary antibody at 4 °C (anti-HIF-1 α 1:500, anti-VEGF 1:500, anti-cleaved caspase-3 1:1,000, and anti-proliferating cell nuclear antigen 1:500). After washing, biotinylated secondary antibody was applied for 30 minutes, followed by streptavidin-horseradish peroxidase complex (Vectastain ABC kit; Vector Labs), DAB solution (DAB kit; Vector Labs), and counterstaining with hematoxylin. Slides were dehydrated, mounted, and viewed. Image-Pro Plus V.4.5 Software (Media Cybernetics, Silver Spring, MD) was used to quantify the positive staining per high-powered field in each section. Three visual fields were evaluated and expressed as the average number of positive cells per high-powered field.

TUNEL and Hoechst 33258 co-staining

TUNEL assay was performed according to the protocol provided by the manufacturer (*In Situ* Cell Death Detection kit, POD; Hoffman La Roche Ltd, Basel, Switzerland). In brief, paraffin-embedded tissue sections were mounted on silanated slides, deparaffinized in xylene, and rehydrated and washed in distilled water. The slides were stripped of protein by digestion with 20 $\mu\text{g ml}^{-1}$ proteinase K in 10 mM Tris-HCl (pH 7.4) at room temperature for 15 minutes. After washing, labeling was performed by covering sections with the TUNEL reaction mixture at 37 °C for 60 minutes. The sections were washed and then overlaid with 0.2 $\mu\text{m ml}^{-1}$ Hoechst 33258 (Sigma-Aldrich) for 1 minute at room temperature for double staining as described previously by von Kobyletzki *et al.* (2000). Slides were washed, mounted, and examined under a fluorescence microscope (Nikon Eclipse E600; Nikon Instruments Inc., Melville, NY) with immediate photography.

DNA electrophoresis

To isolate genomic DNA from wound tissues, the homogenized tissue was incubated with DNA isolation buffer (50 mM Tris-HCl, pH 8.0, 100 mM EDTA, 0.5% SDS) containing 0.5 mg ml^{-1} proteinase K at 55 °C overnight. Phenol and phenol-chloroform-isoamyl alcohol extraction was performed and the DNA in the aqueous phase was precipitated with 3 M sodium acetate. After washing with 70% ethanol, the DNA samples were dissolved in TE buffer (10 mM Tris-HCl, pH 8.0, 1 mM EDTA). The DNA concentration was measured by spectrophotometry. A 500 ng DNA sample per well was loaded onto 1.2% agarose gel containing 2 $\mu\text{g ml}^{-1}$ ethidium bromide, and electrophoresis was conducted at 90 V for 1 hour in 1 \times TBE buffer (90 mM Tris-borate, 2 mM EDTA). The gel was visualized under UV light.

DNA dot-blotting for BrdU quantitation

A novel dot-blotting method for BrdU quantitation was performed as described by Ueda *et al.* (2005). Briefly, the purified DNA was incubated with 10 volumes of 0.4 N NaOH for 30 minutes at room temperature and kept on ice to prevent annealing. The DNA solution was neutralized with an equal volume of 1 M Tris-HCl (pH 6.8), and 100 ng in 5 μl was dot-blotted onto a nitrocellulose membrane and fixed by UV cross-linking (Fisher Scientific, Waltham, MA). The membrane was incubated with BrdU primary antibody (1:2,000) for 1 hour at room temperature. After being washed with TBST, the membrane was incubated with a secondary antibody, and analyzed

by enhanced chemiluminescence. The intensity of each BrdU signal was quantified by densitometric analysis using Kodak software.

Statistical analysis

Data are presented as mean \pm SEM. One-way analysis of variance with *post hoc* comparisons using Tukey's highly significant difference test was used to determine the statistical significance between groups using InStat version 3.0 (GraphPad Software, San Diego, CA). A *P*-value less than 0.05 was considered significant.

CONFLICT OF INTEREST

The authors state no conflict of interest.

ACKNOWLEDGMENTS

We thank Hal K Hawkins, MD, PhD, for assistance with histology and Dr Richard Bruick, who kindly provided the BNip3 antibody. Dr Gould was supported by a Dennis W Jahnigen Career Development Scholars Award.

SUPPLEMENTARY MATERIAL

Supplementary Materials.

Figure S1. Strongly positive proliferating cell nuclear antigen signal was seen in the cell nuclei in the (a, c, and e) epidermis and (b, d, and f) dermis of ischemic wound tissue in all groups at day 7.

Figure S2. Western blot shows phosphoinositide-3 kinase (PI3K) expression in ischemic wound tissue at days 7 and 10.

REFERENCES

- Abidia A, Laden G, Kuhan G, Johnson BF, Wilkinson AR, Renwick PM *et al.* (2003) The role of hyperbaric oxygen therapy in ischaemic diabetic lower extremity ulcers: a double-blind randomised-controlled trial. *Eur J Vasc Endovasc Surg* 25:513-8
- Badr AE, Yin W, Mychaskiw G, Zhang JH (2001) Effect of hyperbaric oxygen on striatal metabolites: a microdialysis study in awake freely moving rats after MCA occlusion. *Brain Res* 916:85-90
- Baidin SA, Ivanov OP, Ivanov MG, Berendeev SN, Gorinova SV (1997) [Hyperbaric oxygenation in the intensive therapy of hypoconjugation neonatal jaundice]. *Anesteziol Reanimatol* July-August:27-30
- Boyd JM, Malstrom S, Subramanian T, Venkatesh LK, Schaeper U, Elangovan B *et al.* (1994) Adenovirus E1B 19 kDa and Bcl-2 proteins interact with a common set of cellular proteins. *Cell* 79:341-51
- Bruick RK (2000) Expression of the gene encoding the proapoptotic Nip3 protein is induced by hypoxia. *Proc Natl Acad Sci USA* 97:9082-7
- Calvert JW, Zhou C, Nanda A, Zhang JH (2003) Effect of hyperbaric oxygen on apoptosis in neonatal hypoxia-ischemia rat model. *J Appl Physiol* 95:2072-80
- Carmeliet P, Dor Y, Herbert JM, Fukumura D, Brusselmans K, Dewerchin M *et al.* (1998) Role of HIF-1 α in hypoxia-mediated apoptosis, cell proliferation and tumour angiogenesis. *Nature* 394:485-90
- Chen D, Li M, Luo J, Gu W (2003) Direct interactions between HIF-1 α and Mdm2 modulate p53 function. *J Biol Chem* 278:13595-8
- Dean JB, Mulkey DK, Garcia AJ III, Putnam RW, Henderson RA III (2003) Neuronal sensitivity to hyperoxia, hypercapnia, and inert gases at hyperbaric pressures. *J Appl Physiol* 95:883-909
- Detmar M, Brown LF, Schon MP, Elicker BM, Velasco P, Richard L *et al.* (1998) Increased microvascular density and enhanced leukocyte rolling and adhesion in the skin of VEGF transgenic mice. *J Invest Dermatol* 111:1-6
- Detmar M, Yeo KT, Nagy JA, Van de Water L, Brown LF, Berse B *et al.* (1995) Keratinocyte-derived vascular permeability factor (vascular endothelial growth factor) is a potent mitogen for dermal microvascular endothelial cells. *J Invest Dermatol* 105:44-50
- Doctor N, Pandya S, Supe A (1992) Hyperbaric oxygen therapy in diabetic foot. *J Postgrad Med* 38:112-4, 111

- Dong H, Xiong L, Zhu Z, Chen S, Hou L, Sakabe T (2002) Preconditioning with hyperbaric oxygen and hyperoxia induces tolerance against spinal cord ischemia in rabbits. *Anesthesiology* 96:907-12
- Dor Y, Porat R, Keshet E (2001) Vascular endothelial growth factor and vascular adjustments to perturbations in oxygen homeostasis. *Am J Physiol Cell Physiol* 280:C1367-74
- Dvorak HF, Brown LF, Detmar M, Dvorak AM (1995) Vascular permeability factor/vascular endothelial growth factor, microvascular hyperpermeability, and angiogenesis. *Am J Pathol* 146:1029-39
- Faglia E, Favales F, Aldeghi A, Calia P, Quarantiello A, Oriani G et al. (1996) Adjunctive systemic hyperbaric oxygen therapy in treatment of severe prevalently ischemic diabetic foot ulcer. A randomized study. *Diabetes Care* 19:1338-43
- Ferrara N, Gerber HP, LeCouter J (2003) The biology of VEGF and its receptors. *Nat Med* 9:669-76
- Galvez AS, Brunskill EW, Marreez Y, Benner BJ, Regula KM, Kirschenbaum LA et al. (2006) Distinct pathways regulate proapoptotic Nix and BNIP3 in cardiac stress. *J Biol Chem* 281:1442-8
- Gillissen A, Nowak D (1998) Characterization of N-acetylcysteine and ambroxol in anti-oxidant therapy. *Respir Med* 92:609-23
- Ginsberg MD (2003) Adventures in the pathophysiology of brain ischemia: penumbra, gene expression, neuroprotection: the 2002 Thomas Willis Lecture. *Stroke* 34:214-23
- Gould LJ, Leong M, Sonstein J, Wilson S (2005) Optimization and validation of an ischemic wound model. *Wound Repair Regen* 13:576-82
- Graham RM, Frazier DP, Thompson JW, Haliko S, Li H, Wasserlauf BJ et al. (2004) A unique pathway of cardiac myocyte death caused by hypoxia-acidosis. *J Exp Biol* 207:3189-200
- Greijer AE, Van der Groep P, Kemming D, Shvarts A, Semenza GL, Meijer GA et al. (2005) Up-regulation of gene expression by hypoxia is mediated predominantly by hypoxia-inducible factor 1 (HIF-1). *J Pathol* 206:291-304
- Greijer AE, van der Wall E (2004) The role of hypoxia inducible factor 1 (HIF-1) in hypoxia induced apoptosis. *J Clin Pathol* 57:1009-14
- Hopf HW, Gibson JJ, Angeles AP, Constant JS, Feng JJ, Rollins MD et al. (2005) Hyperoxia and angiogenesis. *Wound Repair Regen* 13:558-64
- Kairuz E, Upton Z, Dawson RA, Malda J (2007) Hyperbaric oxygen stimulates epidermal reconstruction in human skin equivalents. *Wound Repair Regen* 15:266-74
- Kalani M, Jorneskog G, Naderi N, Lind F, Brismar K (2002) Hyperbaric oxygen (HBO) therapy in treatment of diabetic foot ulcers. Long-term follow-up. *J Diabetes Complicat* 16:153-8
- Kessler L, Bilbault P, Ortega F, Grasso C, Passemar R, Stephan D et al. (2003) Hyperbaric oxygenation accelerates the healing rate of nonischemic chronic diabetic foot ulcers: a prospective randomized study. *Diabetes Care* 26:2378-82
- Kranke P, Bennett M, Roeckl-Wiedmann I, Debus S (2004) Hyperbaric oxygen therapy for chronic wounds. *Cochrane Database Syst Rev* (2):CD004123
- Lamoreaux WJ, Fitzgerald ME, Reiner A, Hasty KA, Charles ST (1998) Vascular endothelial growth factor increases release of gelatinase A and decreases release of tissue inhibitor of metalloproteinases by microvascular endothelial cells *in vitro*. *Microvasc Res* 55:29-42
- Li Y, Zhou C, Calvert JW, Colohan AR, Zhang JH (2005) Multiple effects of hyperbaric oxygen on the expression of HIF-1 alpha and apoptotic genes in a global ischemia-hypotension rat model. *Exp Neurol* 191:198-210
- Mrsic-Pelcic J, Pelcic G, Vitezic D, Antoncic I, Filipovic T, Simonic A et al. (2004) Hyperbaric oxygen treatment: the influence on the hippocampal superoxide dismutase and Na⁺,K⁺-ATPase activities in global cerebral ischemia-exposed rats. *Neurochem Int* 44:585-94
- Murohara T, Horowitz JR, Silver M, Tsurumi Y, Chen D, Sullivan A et al. (1998) Vascular endothelial growth factor/vascular permeability factor enhances vascular permeability via nitric oxide and prostacyclin. *Circulation* 97:99-107
- Nathan C (2002) Points of control in inflammation. *Nature* 420:846-52
- Noiri E, Hu Y, Bahou WF, Keese CR, Giaever I, Goligorsky MS (1997) Permissive role of nitric oxide in endothelin-induced migration of endothelial cells. *J Biol Chem* 272:1747-52
- Ostrowski RP, Colohan AR, Zhang JH (2005) Mechanisms of hyperbaric oxygen-induced neuroprotection in a rat model of subarachnoid hemorrhage. *J Cereb Blood Flow Metab* 25:554-71
- Regula KM, Ens K, Kirshenbaum LA (2002) Inducible expression of BNIP3 provokes mitochondrial defects and hypoxia-mediated cell death of ventricular myocytes. *Circ Res* 91:226-31
- Rosenthal RE, Silbergleit R, Hof PR, Haywood Y, Fiskum G (2003) Hyperbaric oxygen reduces neuronal death and improves neurological outcome after canine cardiac arrest. *Stroke* 34:1311-6
- Seibert K, Masferrer J, Zhang Y, Leahy K, Hauser S, Gierse J et al. (1995) Expression and selective inhibition of constitutive and inducible forms of cyclooxygenase. *Adv Prostaglandin Thromboxane Leukot Res* 23:125-7
- Sheikh AY, Gibson JJ, Rollins MD, Hopf HW, Hussain Z, Hunt TK (2000) Effect of hyperoxia on vascular endothelial growth factor levels in a wound model. *Arch Surg* 135:1293-7
- Shenberger JS, Zhang L, Powell RJ, Barchowsky A (2007) Hyperoxia enhances VEGF release from A549 cells via post-transcriptional processes. *Free Radic Biol Med* 43:844-52
- Siddiqui A, Davidson JD, Mustoe TA (1997) Ischemic tissue oxygen capacitance after hyperbaric oxygen therapy: a new physiologic concept. *Plast Reconstr Surg* 99:148-55
- Sunami K, Takeda Y, Hashimoto M, Hirakawa M (2000) Hyperbaric oxygen reduces infarct volume in rats by increasing oxygen supply to the ischemic periphery. *Crit Care Med* 28:2831-6
- Thom SR (1993) Functional inhibition of leukocyte B2 integrins by hyperbaric oxygen in carbon monoxide-mediated brain injury in rats. *Toxicol Appl Pharmacol* 123:248-56
- Ueda J, Saito H, Watanabe H, Evers BM (2005) Novel and quantitative DNA dot-blotting method for assessment of *in vivo* proliferation. *Am J Physiol Gastrointest Liver Physiol* 288:G842-7
- von Kobyletzki G, Heine O, Stephan H, Pieck C, Stucker M, Hoffmann K et al. (2000) UVA1 irradiation induces deoxyribonuclease dependent apoptosis in cutaneous T-cell lymphoma *in vivo*. *Photodermatol Photoimmunol Photomed* 16:271-7
- Wang GL, Semenza GL (1993) General involvement of hypoxia-inducible factor 1 in transcriptional response to hypoxia. *Proc Natl Acad Sci USA* 90:4304-8
- Wei MC, Zong WX, Cheng EH, Lindsten T, Panoutsakopoulou V, Ross AJ et al. (2001) Proapoptotic BAX and BAK: a requisite gateway to mitochondrial dysfunction and death. *Science* 292:727-30
- Werdich XQ, McCollum GW, Rajaratnam VS, Penn JS (2004) Variable oxygen and retinal VEGF levels: correlation with incidence and severity of pathology in a rat model of oxygen-induced retinopathy. *Exp Eye Res* 79:623-30
- Xiong L, Zhu Z, Dong H, Hu W, Hou L, Chen S (2000) Hyperbaric oxygen preconditioning induces neuroprotection against ischemia in transient not permanent middle cerebral artery occlusion rat model. *Chin Med J (Engl)* 113:836-9
- Yamada H, Yamada E, Hackett SF, Ozaki H, Okamoto N, Campochiaro PA (1999) Hyperoxia causes decreased expression of vascular endothelial growth factor and endothelial cell apoptosis in adult retina. *J Cell Physiol* 179:149-56
- Yasuda M, Theodorakis P, Subramanian T, Chinnadurai G (1998) Adenovirus E1B-19K/BCL-2 interacting protein BNIP3 contains a BH3 domain and a mitochondrial targeting sequence. *J Biol Chem* 273:12415-21
- Yin D, Zhou C, Kusaka I, Calvert JW, Parent AD, Nanda A et al. (2003) Inhibition of apoptosis by hyperbaric oxygen in a rat focal cerebral ischemic model. *J Cereb Blood Flow Metab* 23:855-64
- Yussman MG, Toyokawa T, Odley A, Lynch RA, Wu G, Colbert MC et al. (2002) Mitochondrial death protein Nix is induced in cardiac hypertrophy and triggers apoptotic cardiomyopathy. *Nat Med* 8:725-30
- Zhang JH, Lo T, Mychaskiw G, Colohan A (2005) Mechanisms of hyperbaric oxygen and neuroprotection in stroke. *Pathophysiology* 12:63-77